Unveiling Glutamate Dynamics: Cognitive Demands in Human Short-Term Memory Learning Across Frontal and Parieto-Occipital Cortex: A Functional MRS Study

Hossein Mohammadi (PhD)[1], Shahriyar Jamshidi (PhD)[1], Hassan Khajehpour (PhD)[2], Iman Adibi (MD, PhD)[3,4], Abbas Rahimiforoushani (PhD)[5], Shaghayegh Karimi (PhD)[6], Nasim Dadashi Serej (PhD)[1,7]*, Nader Riyahi Alam (PhD)[6,8,9]*

[1]Department of Bioimaging, School of Advanced Technologies in Medicine, Isfahan University of Medical Sciences (IUMS), Isfahan, Iran
[2]Multimodal Functional Imaging Lab, Department of Physics and PERFORM Centre, Concordia University, Montreal, Quebec, Canada
[3]Department of Neurology, School of Medicine, Isfahan University of Medical Sciences (IUMS), Isfahan, Iran
[4]Isfahan Neurosciences Research Center, Isfahan University of Medical Sciences, Isfahan, Iran
[5]Department of Epidemiology & Biostatistics, School of Public Health, Tehran University of Medical Sciences (TUMS), Tehran, Iran
[6]Department of Medical Physics & Biomedical Eng., School of Medicine, Tehran University of Medical Sciences (TUMS), Tehran, Iran
[7]School of Computing and Engineering, University of West London, UK
[8]Concordia University, PERFORM Center, School of Health, Montreal, Quebec, Canada
[9]Magnetic Resonance Imaging Lab, National Brain Mapping Laboratory (NBML), Tehran, Iran

*Corresponding authors:
Nasim Dadashi Serej
School of Computing and Engineering, University of West London, UK
E-mail: nasim.dadashi-serej@uwl.ac.uk

Nader Riyahi Alam
Concordia University, PERFORM Center, School of Health, Montreal, Quebec, Canada
E-mail: riahialam@gmail.com

Received: 3 July 2024
Accepted: 20 September 2024

ABSTRACT

Background: Acquiring new knowledge necessitates alterations at the synaptic level within the brain. Glutamate, a pivotal neurotransmitter, plays a critical role in these processes, particularly in learning and memory formation. Although previous research has explored glutamate's involvement in cognitive functions, a comprehensive understanding of its real-time dynamics remains elusive during memory tasks.

Objective: This study aimed to investigate glutamate modulation during memory tasks in the right Dorsolateral Prefrontal Cortex (DLPFC) and parieto-occipital regions using functional Magnetic Resonance Spectroscopy (fMRS).

Material and Methods: This experimental research applied fMRS acquisition concurrently with a modified Sternberg's verbal working memory task for fourteen healthy right-handed participants (5 females, mean age=30.64±4.49). The glutamate/total-creatine (Glu/tCr) ratio was quantified by LCModel in the DLPFC and parieto-occipital voxels while applying the tissue corrections.

Results: The significantly higher Glu/tCr modulation was observed during the task with a trend of increased modulation with memory load in both the DLPFC (19.9% higher, *P*-value=0.018) and parieto-occipital (33% higher, *P*-value=0.046) regions compared to the rest.

Conclusion: Our pioneering fMRS study has yielded groundbreaking insights into brain functions during S-term Memory (STM) and learning. This research provides valuable methodological advancements for investigating the metabolic functions of both healthy and disordered brains. Based on the findings, cognitive demands directly correlate with glutamate levels, highlighting the neurochemical underpinnings of cognitive processing. Additionally, the obtained results potentially challenge the traditional left-hemisphere-centric model of verbal working memory, leading to the deep vision of hemispheric contributions to cognitive functions.

Citation: Mohammadi H, Jamshidi Sh, Khajehpour H, Adibi I, Rahimiforoushani A, Karimi Sh, Dadashi Serej N, Riyahi Alam N. Unveiling Glutamate Dynamics: Cognitive Demands in Human Short-Term Memory Learning Across Frontal and Parieto-Occipital Cortex: A Functional MRS Study. *J Biomed Phys Eng*. 2024;14(6):519-532. doi: 10.31661/jbpe.v0i0.2407-1789.

Keywords

Memory, Short-Term; Glutamatergic Agents; Magnetic Resonance Spectroscopy; Learning; Metabolic Brain Mapping

Introduction

Human learning, brain development, and Long-term Memory (LTM) storage depend on Short-term Memory (STM). In the brain, the sensory input information enters the sensory memory.

This is a brief initial stage where sensory information is held for a short period of time also known as the sensory register. If this information is attended to, it transitions into the STM [1, 2]. Learning new information is a mental process facilitated by modifications in the synaptic level among nerve cells that store data. The process, by which neurons connect to networks is primarily facilitated through synaptic plasticity by neurotransmitters of excitatory synapses [3]. Glutamate, the most important excitatory neurotransmitter in human memory and learning, is released in 80% of synapses [4]. Glutamate levels mediate neural network activity in response to stimuli [5]. The relationship between glutamate release, electrical signaling, and metabolic demands is intricate and bidirectional. The function of glutamate-gated N-methyl-D-aspartate (NMDA) receptors is well-established in synaptic plasticity and memory formation. To function as a "coincidence detector," this receptor needs to be activated by both postsynaptic depolarization and presynaptic glutamate release, resulting in a calcium influx and the subsequent intracellular signaling cascades [6]. Glutamate release into the synaptic cleft causes an electrical reaction in the postsynaptic neuron propagating along the neuron, releasing neurotransmitters and continuing neural network activity [7]. The NMDA receptor controls synaptic plasticity and mediates memory and learning. Long-term Potentiation (LTP) or Long-term Depression (LTD), which results from the calcium influx into postsynaptic neurons via the glutamate-gated NMDA receptors, contributes to the establishment of memory [3]. Hence, the measurement of glutamate modulation of neurons could be directly relevant to LTP/LTD, receptor types, depolarization activity, and plasticity during memory formation. The NMDA receptors have a powerful influence on prefrontal cortex function and Working Memory (WM) when afferent stimulation causes neurons to depolarize [8]. During brain activity, the ability to store sensory information for short periods is a key component of WM [9]. Single nerve cells in the frontal cortex can encode the contents of WM by increasing and decreasing activity rapidly [10, 11]. On the other hand, the recall of visual cues is accompanied by a transient increase in glutamate and Gamma-aminobutyric Acid (GABA) concentration levels in the visual cortex [12]. Recent evidence shows that the recruitment of the visual association cortex during encoding is associated with memory performance [13]. Additionally, neurons in the primary visual cortex respond to basic elements of the visual scene and play a role in cognitive processes, including visual perception and working memory [14]. A monkey study found that the primary visual cortex, also involved in vision, displays different activity patterns for images conjured up from memory compared to real-time visual input, showing its crucial role in recalling pictures stored in memory [15]. All these findings highlight the visual cortex's role during memory processing and learning.

The functional Magnetic Resonance Imaging (fMRI) studies have also identified activated brain regions for primary processing and transient storage related to STM for numerical digits in the visual cortex [16, 17]. These findings support the idea that during the formation of a new visual STM, the frontal and posterior regions are involved and communicate. Employing *in-vivo* proton functional Magnetic Resonance Spectroscopy (^{1}H fMRS) in human memory is limited, and investigations were performed mostly on the hippocampus [18, 19] or left Dorsolateral Prefrontal Cortex (DLPFC) [20]. On the other hand, EEG studies have introduced the frontal and parieto-occipital cortices as areas for encoding, storing, and retrieving STM information [21, 22]. Furthermore, a meta-analysis of 42 fMRI studies suggested that the left-hemisphere concept of verbal Working Memory (vWM) should be reconsidered [23]. Therefore, the underlying metabolic function and contribution of the right DLPFC and parieto-occipital cortices

remain unclear in STM. The present study is designed to investigate this gap using verbal STM tasks and fMRS.

Material and Methods

This experimental study is conducted in the following steps.

Participants

The study commenced with the participation of fourteen healthy, right-handed individuals (5 females, mean age=30.64±4.49). Participants were selected from the student population of Tehran universities, Tehran, Iran within the limited age range of 18-35, ensuring a more homogeneous sample, leading to minimizing variability, due to age-related changes in brain metabolism. Health conditions were assessed according to a Structured Clinical Interview for DSM-IV (SCID) and medical history. The volunteers had no history of neurological ailments, psychiatric and mental problems, brain surgeries, or diseases of the brain. Participants who consumed alcohol, smoked, or used drugs were also excluded from the study. Detailed information regarding eating habits, sleep patterns, exercise routines, and work-related stress was collected through well-designed questionnaires. These lifestyle factors were considered, due to their potential impact on brain metabolites. All volunteers had normal or corrected-to-normal vision, ensuring consistent visual perception during the study. This study was approved by the local ethics committee at Isfahan University of Medical Sciences, Isfahan, Iran. The committee reviewed the study protocol, consent forms, and all related documents to ensure compliance with ethical standards and guidelines. Participants were provided detailed information about the study, including its purpose, procedures, potential risks, and benefits. Written informed consent was obtained from all participants before their inclusion in the study.

Experimental Design

This study used a modified version of Sternberg's verbal short-term memory task. The task, depicted in Figure 1a, comprised four phases: encoding, retention, response, and rest. During the encoding phase, participants were presented with a random sequence of

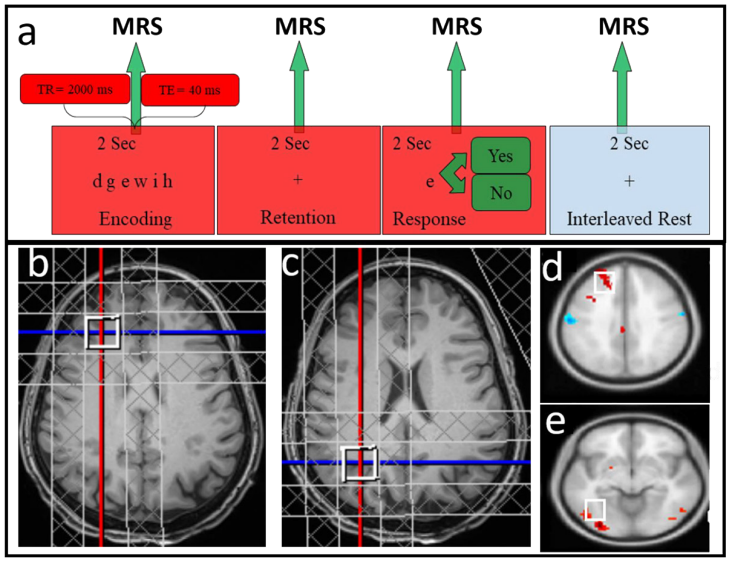

Figure 1: A modified Sternberg's verbal working memory task (**a**): Magnetic resonance spectroscopy voxel placement in the DLPFC (dorsolateral prefrontal cortex) (**b**) and parieto-occipital cortex (**c**). The BOLD (blood-oxygen-level-dependent) signal confirmed the activation of target areas: right dorsolateral prefrontal (**d**) and parieto-occipital (**e**) cortices.

letters they were instructed to memorize. Displaying a cross signified the retention phase. In the response phase, a single letter was displayed, and the participants were instructed to respond as quickly and accurately as possible. The response time was measured from stimulus onset to a button press (in seconds). Each part of the trial precisely lasted two seconds. The fMRS acquisition was concurrently initiated with the commencement of the task display using a trigger box.

MRI and fMRS Data Acquisitions Setup and Measurements

Magnetic Resonance Imaging (MRI) and fMRS measurements were acquired using a 3 Tesla MR scanner with a 64-channel hydrogen head and neck coil (MAGNETOM Prisma, Siemens Healthineers, Erlangen, Germany) at the National Brain Mapping Laboratory (NBML) of Iran (https://nbml.ir/). All acquisitions were performed in the morning between 10 a.m. and 12 p.m. No acquisitions were conducted before the current study to minimize the thermal frequency drift effect on MRS spectra. High-resolution 3D T1-weighted images were acquired using a Magnetization-prepared Rapid Gradient-echo (MPRAGE) sequence (field of view=250 mm^2, voxel size=1×1×1 mm^3, Repetition Time (TR)=1800 ms, Echo Time (TE)=3.5 ms, Inversion Time (TI)=1100 ms, flip angle=7°, averages=1, number of slices=176) in the sagittal plane.

The fMRS acquisition was performed following a static shimming using a localized voxel adjusted on the right DLPFC [24], and right parieto-occipital cortex (Figure 1), utilizing the Point RESolved Spectroscopy (PRESS) sequence (voxel size=20×20×20 mm^3, TR=2000 ms, TE=40 ms. The TE of 40 ms in 3T ^{1}H-MRS using the PRESS sequence led to the reliable measurement of glutamate by reducing the glutamine overlapping signal and yielding the lowest Cramer-Rao Lower Bounds (CRLB) for glutamate quantification spectra [25]. The "save single average" option was activated to have separate spectra for each part of the task. The MRS voxel was placed on the DLPFC manually, bounded by the superior-lateral extension of the cerebrum, the right middle frontal gyrus, the precentral sulcus, and the superior frontal sulcus. The Parieto-occipital Sulcus (POS) was a crucial landmark for voxel placement in the parieto-occipital cortex (Figure 1). Manual placement can cause voxel placement to adjust based on the participant's anatomical variations or functional considerations. To prevent lipid contamination in spectra, the scalp was avoided while adjusting the MRS voxel, and saturation bands were applied to all six borders of the voxel for outer volume saturation.

The fMRS acquisition first started without any task, in a resting state by looking at a cross in the center of the screen (continuous rest). In the next step, the presentation of the task and fMRS acquisition were executed simultaneously. The fMRS acquisitions were performed in a fixed order, i.e., first from the right DLPFC and then from the right parieto-occipital cortex. This fixed order ensures uniformity across subjects and minimizes potential confounds due to order effects. The TR of the PRESS sequence was equal to the time of each presentation (2000 ms), so for every phase of the task, we have separate spectra. This resulted in 96 spectra for 96 presentations, i.e., 24 trials, and each trial had 4 presentations (encoding, retention, response, and rest, so 4×24=96) in every fMRS acquisition. At the end of each run, the water-unsuppressed signals from the same voxel were acquired so we could perform water scaling. Therefore, we had four metabolite spectra acquisitions (1 at rest and 3 during the tasks) and one water-unsuppressed spectra acquisition, resulting in a total of five acquisitions for each voxel location, resulting in 960 (10×96) spectra and 15 minutes and 10 seconds of data acquisition for each voxel. This led to an overall examination time of 30 minutes and 20 seconds for each subject.

Right after performing the fMRS recording, the DLPFC and parieto-occipital cortex activation were confirmed using fMRI (Reference scan mode=Echo Planar Imaging (EPI)/ separate, TR=2000 ms, and TE=30 ms) signal while running the task (Figure 1d-e).

MRI and MRS Data Analysis

Tissue Volume Segmentation

MRI structural T1-weighted images were segmented based on tissue types using FMRIB Software Library (FSL) software version 6.0.7. The snapshot was captured from the location of the MRS voxel during data acquisition served as a valuable reference for verifying the actual voxel segmentation. The skull was removed using Brain Extraction Tool (BET) functionality. Segmentation and partial volume correction were performed using the Hitchhiker's Guide [26]. The FMRIB's Automated Segmentation Tool (FAST) option was used to extract Partial Volume Estimate (PVE) maps of Cerebrospinal Fluid (CSF), Gray Matter (GM), and White Matter (WM). PVE images are the most accurate way of calculating tissue volumes [27]. The tissues inside the MRS voxel were segmented using a binary mask created by MATLAB (version 2018b). MATLAB is a powerful and versatile tool for advanced image processing. The partial volume calculations proceeded for tissues inside the MRS voxel (Figure 2B-C) using FSL. The composition of tissues inside the MRS voxels is reported in Table 1. These calculations were used in the next step for tissue correction.

MRS Spectrum Processing and Quantification

Spectra, which did not meet the quality criteria, were excluded from the analysis; for example, the CRLB higher than 25%. The average Full-width-at-half-maximum (FWHM) of the spectra was 12.3±2.4 Hz (varied between 9.9 and 14.7 Hz). The MRS spectra were analyzed using the LCModel (version 6.3-1R), which uses an automated algorithm and simulated basis set to quantify the metabolite concentration [28]. This technique is suitable for estimating overlapped metabolite signals, such as glutamate and glutamine. The spectra were tissue and relaxation time corrected as described previously [26], using the "Water Concentration (WCONC)" term calculated for each VOI using equation (1):

$$WCONC = \frac{[H_2O]\left(\left(f_{GM}R_{H_2O_{GM}}\right)+\left(f_{WM}R_{H_2O_{WM}}\right)+\left(f_{CSF}R_{H_2O_{CSF}}\right)\right)}{1-f_{csf}} \quad (1)$$

WCONC is the visible water concentration (mM) inside the voxel, with unit of the fractional brain water content in the voxel (β_{MR}), which is 55556 β_{MR} for CSF [29]. The f_{gm}, f_{wm}, and f_{csf} are the water fractions in each tissue type, calculated by equation (2):

$$f_X = \frac{C_X V_X}{0.82v_{GM} + 0.73v_{WM} + 0.98v_{CSF}} \quad (2)$$

where C_X is expressed as water content fractions in GM, WM, and CSF, which are 0.82, 0.73, and 0.98, respectively. The factor $1/(1-f_{csf})$ in equation (1) is the partial-volume correction. Considering that the metabolites are concentrated in gray matter and white matter, this factor corrects for this fact. V_X is the fraction of the segmented tissue in the MRS voxel. The $R_{H_2O_X}$ is the relaxation factor, based on the fact that water relaxes inside different tissues at different rates [30] and computed using equation (4):

$$R_{H_2O_X} = e^{\frac{-TE}{T2_X}}\left(1-e^{\frac{-TR}{T1_X}}\right) \quad (3)$$

where T1 and T2 are the water relaxation times in the tissue type X, and the TR and TE are the time to repeat and time to echo. To account for the blood-oxygen-level-dependent (BOLD) effect [31], which may inflate the metabolite levels, the metabolites were normalized to the total creatine level, which is similarly affected by the BOLD effect [4] and remains constant under normal physiological conditions.

Statistical Analysis

Statistical analysis was performed using

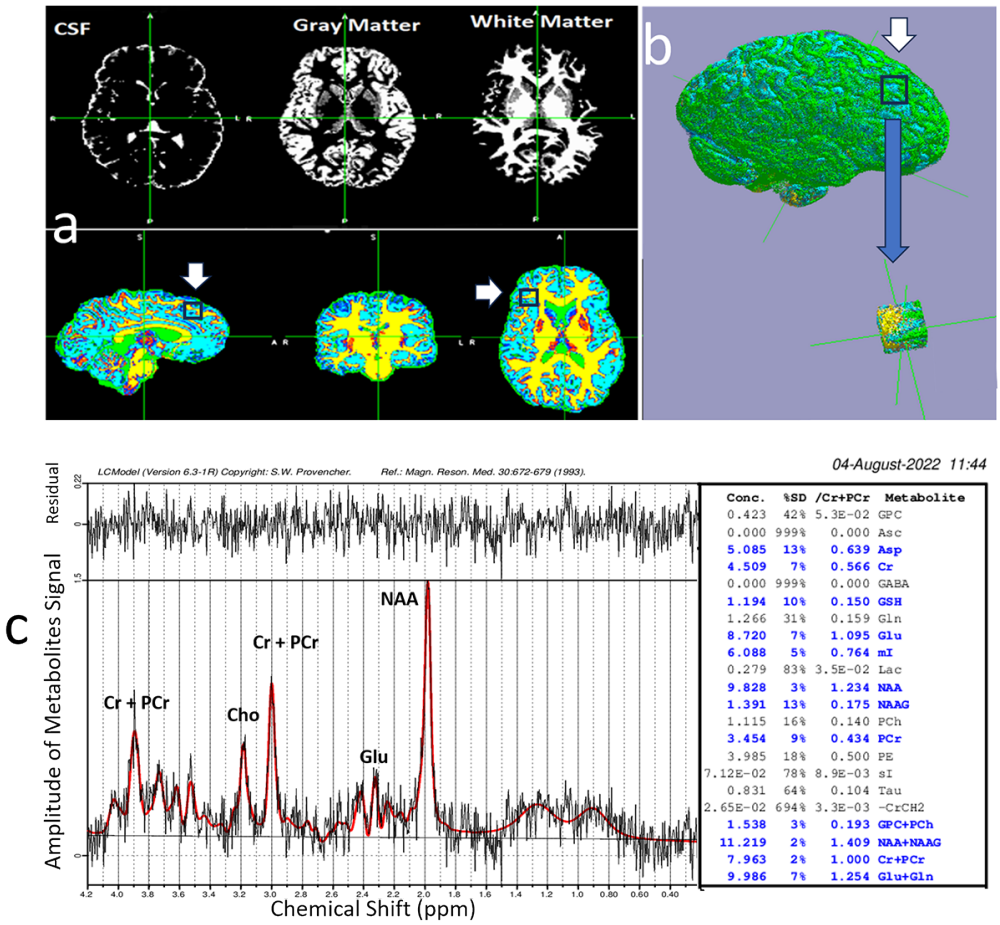

Figure 2: (**a**) Partial volume segmentation of brain tissues into three classes: cerebrospinal fluid, gray matter, and white matter (upper row). Mixed and colored brain tissues are displayed in the lower row in sagittal, coronal, and axial views (left to right, respectively). 3D representation of segmented tissues inside the volume of interest in the dorsolateral prefrontal cortex that its location annotated by a black arrow, compared to the whole brain **(b)**. **(c)** Left: showing a sample spectrum acquired in a single time to repeat (single event, for example, Encoding) and quantified using a linear combination model. The black line is the original signal, the red line is the LC Model estimation of simulated metabolites and the black line above is residual. **(c)** Right: Conc. representing metabolites concentration in millimolars. SD (standard deviation) identifying Cramer-Rao lower bounds (CRLBs) in %. The third column is the metabolite concentrations normalized to total creatine. The blue colors identify the lowest CRLBs.

Table 1: Mean tissue volume composition of magnetic resonance spectroscopy voxels (%)

VOI (volume of interest)	Gray Matter	White Matter	Cerebrospinal Fluid
DLPFC (dorsolateral prefrontal cortex)	0.39±0.05	0.43±0.04	0.18±0.03
Parieto-Occipital	0.41±0.03	0.37±0.02	0.22±0.02

IBM SPSS Statistics (v27.0.1.0, 2020, SPSS, Inc., an IBM Company, Chicago, United States of America). The Kruskal-wallis test was used to determine, whether there was a statistically significant difference between the medians of groups. The participants were split into two groups of fast and slow learners based on the median split of response time. Considering the non-normal distribution and limited data sample, a nonparametric paired Mann-Whitney test was performed to evaluate whether the response time and percentage of correct answers were differed by learning subgroups to indicate learning rate and asymptotic performance. Variables for this test included task condition, response time, and accuracy. A one-way repeated measure of the analysis of variance (rmANOVA) test, followed by a post-hoc test with the Bonferroni correction was employed to examine the main effect of memory load on accuracy and response time.

To determine if Glu/tCr ratios varied significantly either during memory loads compared to continuous rest, or across different task conditions, a one-way rmANOVA was conducted for each region of interest (ROI). This was followed by a post-hoc test using the Bonferroni correction.

Results

Behavioral Results

Participants responded with an average accuracy of 96%. Accuracy decreased with an increase in the memory load (Figure 3b). The lists of 2, 4, and 6-letter sets had accuracy rates of 98.89%±1.52%, 96.39%±2.07%, and 88.93%±6.74%, and response times of 0.93±0.50 seconds, 1.03±0.66 seconds, and 1.11±0.73 seconds, respectively (Figure 3b). There was a significant effect of memory loads on the means of response time ($F_{(2, 26)}$=7.22, *P*-value=0.006, η_p^2=0.357) and accuracy ($F_{(2, 26)}$=27.64, *P*-value<0.001, η_p^2=0.680). Post-hoc tests indicated that the response time for the 6-letter set was significantly longer than in 2-letter (*P*-value=0.001) and 4-letter sets (*P*-value=0.032), but there was no significant difference between 2- and 4-letter sets. Accuracy in the 6-letter set was significantly lower than in the 2-letter

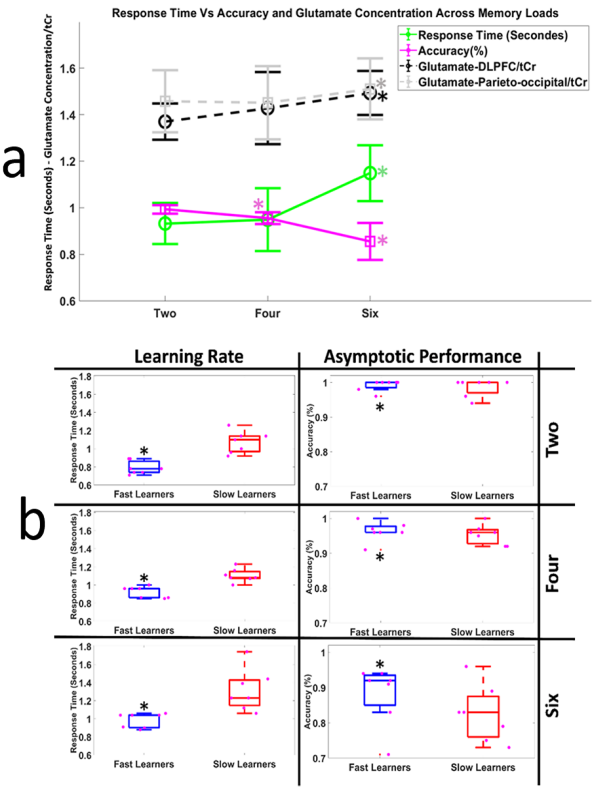

Figure 3: a: One-way rmANOVA to compare the effect of memory loads on dependent variables. A significant effect was found in response time ($F_{(2, 26)}$=7.22, *P*-value=0.006, η_p^2=0.357), accuracy ($F_{(2, 26)}$=27.64, *P*-value<0.001, η_p^2=0.680) and glutamate/total creatine ratio in the DLPFC ($F_{(3, 39)}$=4.16, *P*-value=0.043, η_p^2=0.243) and parieto-occipital ($F_{(3, 39)}$=6.41, *P*-value=0.006, η_p^2=0.330). **b**: Learning rate and asymptotic performance differed significantly (*) between fast and slow learners across all memory loads. Fast learners responded quicker and had higher accuracy, indicating learning rate and asymptotic performance were related directly.

(*P*-value=0.023) and 4-letter sets (*P*-value=0.022) and significantly lower in the 4-letter set than in the 2-letter set (*P*-value=0.009) (Figure 3a).

The participants cleaved into fast (age=31±1.73) and slow (age=30.28±6.36) learners (n=7 in each). Mann-whitney results indicated that fast learners had significantly lower response times in the 2-letter (Z=-9.054, *P*-value<0.001), 4-letter (Z=-9.063, *P*-value<0.001), and 6-letter (Z=-9.096, *P*-value<0.001) sets, respectively, and higher accuracy than slow learners in the 2-letter (Z=-3.573, *P*-value<0.001), 4-letter (Z=-2.033, *P*-value=0.042), and 6-letter sets (Z=-4.799, *P*-value<0.001). Fast learners responded quicker and had higher accuracy, indicating a direct relationship between learning rate and asymptotic performance.

^{1}H fMRS Results

Glutamate concentration in millimolar (mM) was normalized to total creatine concentration (tCr) in mM (reported here in relative form (Glu/tCr)). A significant effect of memory loads on the Glu/tCr was found in the DLPFC ($F_{(3, 39)}$=4.16, *P*-value=0.043, η_p^2=0.243) and parieto-occipital ($F_{(3, 39)}$=6.41, *P*-value=0.006, η_p^2=0.330) voxel. Post-hoc analysis indicated significantly higher Glu/tCr modulation in the memory load of the 6-letter set than in continuous rest in both the DLPFC (19.90% higher, *P*-value=0.018) and parieto-occipital (33.00% higher, *P*-value=0.046) and no significant difference between other memory loads in either target area (Figure 4). Glu/tCr levels across task conditions during each memory load are described as follows: 1) memory load of the 2-letter set: the rmANOVA showed that there was no significant effect of task condition on the Glu/tCr ratio in the DLPFC voxel ($F_{(4, 52)}$=2.67, *P*-value=0.067, η_p^2=0.171). However, task conditions significantly affected Glu/tCr levels in the parieto-occipital voxel ($F_{(4, 52)}$=5.98, *P*-value=0.007,

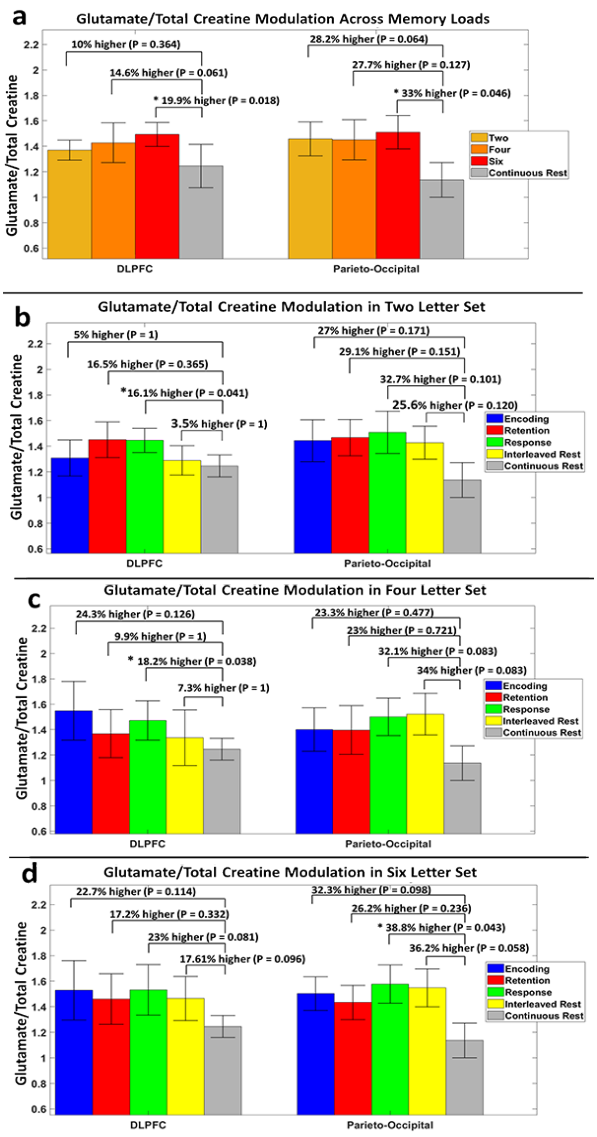

Figure 4: The mean task-related glutamate/total creatine (Glu/tCr) concentration ratio in each memory load for both target regions indicated higher glutamate levels during tasks compared to continuous rest. Glutamate levels increased with memory load **(a)**. Modulation of glutamate across task and rest conditions are displayed **(b-d)**. Elevated Glu/tCr levels were found to be significant compared to continuous rest in the response phase in the memory load of the 2-letter set (*P*=0.041) and 4-letter set (*P*=0.038) in the DLPFC, and 6-letter set (*P*=0.043) in the parieto- occipital (A, B, and C respectively).

η_p^2=0.315). The post-hoc test showed a significantly higher glutamate level in the response phase than in continuous rest in the DLPFC (16.10% higher, *P*-value=0.041). No significant differences were found between any pairs of task conditions in the parieto-occipital voxel. The rest of the *P*-values are annotated in Figure 4; 2) memory load of the 4-letter set: there was no significant effect of task condition on Glu/tCr levels in the DLPFC voxel ($F_{(4, 52)}$=2.59, *P*-value= 0.065, η_p^2=0.166), while the same measure indicated a significant effect for the parieto-occipital voxel ($F_{(4, 52)}$=5.85, *P*-value= 0.011, η_p^2=0.310). No significant differences were found between any pairings of task conditions using post-hoc analysis, and 3) memory load of the 6-letter set: a significant effect of task condition on Glu/tCr modulation was observed in both the DLPFC ($F_{(4, 52)}$=3.38, *P*-value=0.042, η_p^2=0.207) and parieto-occipital ($F_{(4, 52)}$=8.56, *P*-value=0.003, η_p^2=0.397) voxels. No significant differences were observed between Glu/tCr levels of task conditions in the DLPFC using pairwise comparisons by post-hoc analysis, while these measures were significant in the parieto-occipital in a way that Glu/tCr levels higher in the response than in the retention (*P*-value=0.024) and continuous rest (*P*-value=0.043).

The Mann-Whitney test in learning subgroups indicated no significant differences in Glu/tCr concentration for the memory load of 2-letter (Z=-1.27, *P*-value=0.201), 4-letter (Z=-1.07, *P*-value=0.283), and 6-letter (Z=-0.91, *P*-value=0.363) sets in the DLPFC. Also, the same measurements for the parieto-occipital were not significant in the memory load of 2-letter (Z=-0.10, *P*-value=0.915), 4-letter (Z=-1.25, *P*-value=0.210), and 6-letter (Z=-0.23, *P*-value=0.812) sets.

Discussion

Glutamate, glutamate-regulated neural firing, subsequent glutamate release, and the repetition of this cycle are a complex interplay essential for STM and learning [7]. In addition, frontal and prieto-occipital cortices are involved in WM and retrieval [32, 33]. However, the glutamate modulation of the right DLPFC and parieto-occipital cortex during STM remains a case, which is addressed in this study using fMRS. The right DLPFC is involved in higher-order cognitive processes, such as working memory, cognitive flexibility, and attentional control. Additionally, the DLPFC is implicated in memory-guided attention, due to its role in memory-based biases during visual processing [34, 35]. The prieto-occipital cortices are structural and functional hubs in the brain, participating in the default mode network and executive control network [36]. The right DLPFC and the right posterior parietal cortex have been associated with memory-guided attention [37]. The current study emphasizes the role of glutamate content in the DLPFC and the parieto-occipital cortices as a shared property that may contribute to top-down attentional control and visual processing tasks.

The glutamine-glutamate cycling and neuronal glucose oxidation relationship is estimated at approximately 1:1 [25]. The neurotransmitter pool of glutamate and metabolic processes are coupled and indistinguishable [38]. In addition, neural activity increases with memory consolidation causing glucose consumption and oxidative metabolism to increase, which itself includes the glutamate and glutamine cycle [18]. On the other hand, neuroplasticity, which is crucial for learning and memory, is mainly more related to glutamate rather than glutamine [39]. Moreover, the combined measurement of glutamate and glutamine (Glx) did not reveal significant changes with learning measures [19]. Therefore, to meaningfully observe neuronal plasticity, an attempt should be made to measure the signal of glutamate rather than glutamine. To minimize the overlap of glutamate and glutamine signals, a PRESS sequence with a TE of 40 ms was

used, as suggested in previous studies [40, 41]. The LCModel software was then employed to quantify glutamate and glutamine separately by estimating overlapping resonances and correcting for relaxation time and partial volume effects.

Previous studies suggest that glutamate plays a significant role in mediating sensory information processing and sensorimotor integration during various tasks [42, 43]. Significantly higher modulation of glutamate was observed during the Sternberg's task. In the current study, the obtained results were consistent with the elevated glutamate levels in the left DLPFC during the letter 2-back task [20]. Similarly, glutamate concentration increased significantly during sensory-guided tasks compared to rest in the dorsolateral and arcuate areas of the prefrontal cortex in primates [44]. Additionally, increased glutamate is associated with a reduction in default mode network deactivation in the human brain's posterior cingulate cortex/precuneus [45]. Furthermore, the present research showed a more noticeable increase in glutamate in the DLPFC during the response phase, showing prefrontal cortex neurons play a larger role in retrieval. Accordingly, the synthesis of glutamate is necessary to carry out a learning cycle, or the presence of glutamate is necessary for retrieving a newly formed memory.

Evidence indicates that WM capacity impacts cognitive processing and learning outcomes [46]. Furthermore, increasing memory load led to greater BOLD activation in the prefrontal and parietal cortices [47] and decreased activity in the hippocampus [48]. However, one study indicated no load sensitivity in DLPFC Glx levels [49]. Surveying glutamate levels under various loads, which has not been completely examined, increases the understanding of its function and associated electrical oscillations during cognition. The present study showed that increasing memory load can lead to decreasing accuracy and increasing the glutamate concentration. Hence, it can be concluded that the synthesis of glutamate is essential not only for successful retrieval, but also for the very nature of learning and memory retrieval. This is particularly true under higher memory loads, even though it may result in a higher number of incorrect answers.

The NMDA dysfunction is implicated in a variety of neuropsychiatric disorders, including Alzheimer's, schizophrenia, depression, ischemic brain injury, and chronic pain [50]. Investigating the role of NMDA using fMRS or in combination with other modalities, such as EEG, can help identify potential therapeutic targets for memory disorders. Additionally, research on non-ill individuals, who have memory impairments, may help clarify the processes underlying the condition and identify possible indicators for early detection and treatment. For example, the abnormality of glutamate transmission induced by the NMDA hypofunction is causally associated with the symptoms of schizophrenia [51].

The present method has not been able to distinguish between intracellular and extracellular glutamate yet. Hertz and Rothman have reported that intracellular glutamine is transformed into glutamate, which is subsequently secreted into the synaptic cleft, resulting in either LTD or LTP [52]. The residual glutamate is then converted into glutamine and stored in the presynaptic neuron. Therefore, future studies can be designed to investigate the distinction between intracellular and extracellular glutamate or in combination with other methods like EEG.

Conclusion

The outcome of this research indicates that the right DLPFC and parieto-occipital cortices emerge as key players, with glutamate modulation influencing attentional control and visual processing. The findings underscore the essential role of glutamate synthesis in learning cycles and the retrieval of newly formed memories, providing valuable

methodological advancements for investigating the metabolic functions of both healthy and disordered brains. Additionally, our results suggest a direct correlation between cognitive demands and glutamate levels, highlighting the neurochemical underpinnings of cognitive processing. These insights challenge the traditional left-hemisphere-centric model of verbal working memory, suggesting a more nuanced understanding of hemispheric contributions to cognitive functions. Future investigations could explore glutamate dynamics in combination with other methods to further elucidate these complex processes.

Acknowledgment

I would especially like to thank Dr. Nasim Dadashiserej and Prof. Nader Riyahi Alam, who have been my main mentors for providing the idea of the research, and for their unwavering support. Drs. Iman Adibi and Abbas Rahimiforoushani, who served as my counselors in neurology and biostatistical analysis, also have my sincere gratitude. We value Mrs. Shaghayegh Karimi's unceasing efforts in gathering data in the laboratory. Finally, I would like to thank my friend and fellow student, Mr. Shahriyar Jamshidi, for his assistance in finding volunteers who met the inclusion and exclusion criteria.

Authors' Contribution

The idea for the study was conceived by N. Dadashi and N. Riyahi Alam, while H. Mohammadi and Sh. Jamshidi gathered the related literature. H. Mohammadi, Sh. Jamshidi, and Sh. Karimi implemented the method. H. Mohammadi performed MRS spectrum analysis, while H. Khajeh Pour and H. Mohammadi wrote the methods section. I. Adibi illustrated the targeting of related areas of the brain and brain functioning during the task. A. Rahimi guided and consulted on the statistical analysis. N. Dadashi and N. Riyahi Alam proofread and supervised the research work. All authors read, modified, and approved the final version of the manuscript.

Ethical Approval

This study was approved by the local ethics committee at Isfahan University of Medical Sciences, Isfahan, Iran (Code of ethics: IR.MUI.RESEARCH.REC.1400.381) and the National Brain Mapping Laboratory (NBML) of Iran (https://nbml.ir/).

Informed Consent

This study adhered to the institutional research committee's ethical requirements in all human subject procedures. Every individual participant participating in the study gave informed consent.

Funding

This study was supported by Isfahan University of Medical Sciences, Isfahan [grant number: 3400708].

Conflict of Interest

None

References

1. Kumaran D. Short-term memory and the human hippocampus. *J Neurosci.* 2008;**28**(15):3837-8. doi: 10.1523/JNEUROSCI.0046-08.2008. PubMed PMID: 18400882. PubMed PMCID: PMC6670459.
2. Atkinson RC, Shiffrin RM. Human memory: A proposed system and its control processes. *Psychology of Learning and Motivation*. 1968;**2**:89-195. doi: 10.1016/S0079-7421(08)60422-3.
3. Kennedy MB. Synaptic Signaling in Learning and Memory. *Cold Spring Harb Perspect Biol.* 2013;**8**(2):a016824. doi: 10.1101/cshperspect.a016824. PubMed PMID: 24379319. PubMed PMCID: PMC4743082.
4. Lally N, Mullins PG, Roberts MV, Price D, Gruber T, Haenschel C. Glutamatergic correlates of gamma-band oscillatory activity during cognition: a concurrent ER-MRS and EEG study. *Neuroimage*. 2014;**85**:823-33. doi: 10.1016/j.neuroimage.2013.07.049. PubMed PMID: 23891885.
5. Magistretti PJ, Pellerin L, Rothman DL, Shulman RG. Energy on demand. *Science.* 1999;**283**(5401):496-7. doi: 10.1126/science.283.5401.496. PubMed PMID: 9988650.

6. Reiner A, Levitz J. Glutamatergic Signaling in the Central Nervous System: Ionotropic and Metabotropic Receptors in Concert. *Neuron.* 2018;**98**(6):1080-98. doi: 10.1016/j.neuron.2018.05.018. PubMed PMID: 29953871. PubMed PMCID: PMC6484838.
7. Pal MM. Glutamate: The Master Neurotransmitter and Its Implications in Chronic Stress and Mood Disorders. *Front Hum Neurosci.* 2021;**15**:722323. doi: 10.3389/fnhum.2021.722323. PubMed PMID: 34776901. PubMed PMCID: PMC8586693.
8. Castner SA, Williams GV. Tuning the engine of cognition: a focus on NMDA/D1 receptor interactions in prefrontal cortex. *Brain Cogn.* 2007;**63**(2):94-122. doi: 10.1016/j.bandc.2006.11.002. PubMed PMID: 17204357.
9. D'Esposito M. From cognitive to neural models of working memory. *Philos Trans R Soc Lond B Biol Sci.* 2007;**362**(1481):761-72. doi: 10.1098/rstb.2007.2086. PubMed PMID: 17400538. PubMed PMCID: PMC2429995.
10. Miller EK, Erickson CA, Desimone R. Neural mechanisms of visual working memory in prefrontal cortex of the macaque. *J Neurosci.* 1996;**16**(16):5154-67. doi: 10.1523/JNEUROSCI.16-16-05154.1996. PubMed PMID: 8756444. PubMed PMCID: PMC6579322.
11. Romo R, Brody CD, Hernández A, Lemus L. Neuronal correlates of parametric working memory in the prefrontal cortex. *Nature.* 1999;**399**(6735):470-3. doi: 10.1038/20939. PubMed PMID: 10365959.
12. Koolschijn RS, Shpektor A, Clarke WT, Ip IB, Dupret D, Emir UE, Barron HC. Memory recall involves a transient break in excitatory-inhibitory balance. *Elife.* 2021;**10**:e70071. doi: 10.7554/eLife.70071. PubMed PMID: 34622779. PubMed PMCID: PMC8516417.
13. Rosen ML, Sheridan MA, Sambrook KA, Peverill MR, Meltzoff AN, McLaughlin KA. The Role of Visual Association Cortex in Associative Memory Formation across Development. *J Cogn Neurosci.* 2018;**30**(3):365-80. doi: 10.1162/jocn_a_01202. PubMed PMID: 29064341. PubMed PMCID: PMC5792361.
14. Super H. Working memory in the primary visual cortex. *Arch Neurol.* 2003;**60**(6):809-12. doi: 10.1001/archneur.60.6.809. PubMed PMID: 12810483.
15. Nowogrodzki J. How the 'mind's eye' calls up visual memories from the brain. *Nature.* 2024;**630**(8018):802. doi: 10.1038/d41586-024-01757-3. PubMed PMID: 38877220.
16. Nie J, Zhang Z, Wang B, Li H, Xu J, Wu S, et al. Different memory patterns of digits: a functional MRI study. *J Biomed Sci.* 2019;**26**(1):22. doi: 10.1186/s12929-019-0516-y. PubMed PMID: 30832663. PubMed PMCID: PMC6398246.
17. Attout L, Fias W, Salmon E, Majerus S. Common neural substrates for ordinal representation in short-term memory, numerical and alphabetical cognition. *PLoS One.* 2014;**9**(3):e92049. doi: 10.1371/journal.pone.0092049. PubMed PMID: 24632823. PubMed PMCID: PMC3954845.
18. Stanley JA, Burgess A, Khatib D, Ramaseshan K, Arshad M, Wu H, Diwadkar VA. Functional dynamics of hippocampal glutamate during associative learning assessed with in vivo 1H functional magnetic resonance spectroscopy. *Neuroimage.* 2017;**153**:189-97. doi: 10.1016/j.neuroimage.2017.03.051. PubMed PMID: 28363835. PubMed PMCID: PMC5498221.
19. Spurny B, Seiger R, Moser P, Vanicek T, Reed MB, Heckova E, Michenthaler P, et al. Hippocampal GABA levels correlate with retrieval performance in an associative learning paradigm. *Neuroimage.* 2020;**204**:116244. doi: 10.1016/j.neuroimage.2019.116244. PubMed PMID: 31606475. PubMed PMCID: PMC7610791.
20. Woodcock EA, Anand C, Khatib D, Diwadkar VA, Stanley JA. Working Memory Modulates Glutamate Levels in the Dorsolateral Prefrontal Cortex during 1H fMRS. *Front Psychiatry.* 2018;**9**:66. doi: 10.3389/fpsyt.2018.00066. PubMed PMID: 29559930. PubMed PMCID: PMC5845718.
21. Emad-Ul-Haq Q, Hussain M, Aboalsamh H, Bamatraf S, Malik AS, Amin HU. A Review on understanding Brain, and Memory Retention and Recall Processes using EEG and fMRI techniques [Internet]. arXiv [Preprint]. 2019 [cited 2019 April 30]. Available from: https://arxiv.org/abs/1905.02136.
22. Boly M, Massimini M, Tsuchiya N, Postle BR, Koch C, Tononi G. Are the Neural Correlates of Consciousness in the Front or in the Back of the Cerebral Cortex? Clinical and Neuroimaging Evidence. *J Neurosci.* 2017;**37**(40):9603-13. doi: 10.1523/JNEUROSCI.3218-16.2017. PubMed PMID: 28978697. PubMed PMCID: PMC5628406.
23. Emch M, Von Bastian CC, Koch K. Neural Correlates of Verbal Working Memory: An fMRI Meta-Analysis. *Front Hum Neurosci.* 2019;**13**:180. doi: 10.3389/fnhum.2019.00180. PubMed PMID: 31244625. PubMed PMCID: PMC6581736.
24. Mohammadi H, Changizi V, Riyahi Alam N, Rahiminejad F, Soleimani M, Qardashi A. Measurement of Post-Treatment Changes in Brain Me-

tabolites in Patients with Generalized Anxiety Disorder using Magnetic Resonance Spectroscopy. *J Biomed Phys Eng.* 2022;**12**(1):51-60. doi: 10.31661/jbpe.v0i0.1224. PubMed PMID: 35155293. PubMed PMCID: PMC8819263.

25. Rothman DL, Behar KL, Hyder F, Shulman RG. In vivo NMR studies of the glutamate neurotransmitter flux and neuroenergetics: implications for brain function. *Annu Rev Physiol.* 2003;**65**:401-27. doi: 10.1146/annurev.physiol.65.092101.142131. PubMed PMID: 12524459.
26. Quadrelli S, Mountford C, Ramadan S. Hitchhiker's Guide to Voxel Segmentation for Partial Volume Correction of In Vivo Magnetic Resonance Spectroscopy. *Magn Reson Insights.* 2016;**9**:1-8. doi: 10.4137/MRI.S32903. PubMed PMID: 27147822. PubMed PMCID: PMC4849426.
27. Zhang Y, Brady M, Smith S. Segmentation of brain MR images through a hidden Markov random field model and the expectation-maximization algorithm. *IEEE Trans Med Imaging*. 2001;**20**(1):45-57. doi: 10.1109/42.906424. PubMed PMID: 11293691.
28. Provencher SW. Estimation of metabolite concentrations from localized in vivo proton NMR spectra. *Magn Reson Med.* 1993;**30**(6):672-9. doi: 10.1002/mrm.1910300604. PubMed PMID: 8139448.
29. Ernst T, Kreis R, Ross BD. Absolute quantitation of water and metabolites in the human brain. I. Compartments and water. *Journal of Magnetic Resonance, Series B.* 1993;**102**(1):1-8. doi: 10.1006/jmrb.1993.1055.
30. Bansal R, Hao X, Liu F, Xu D, Liu J, Peterson BS. The effects of changing water content, relaxation times, and tissue contrast on tissue segmentation and measures of cortical anatomy in MR images. *Magn Reson Imaging*. 2013;**31**(10):1709-30. doi: 10.1016/j.mri.2013.07.017. PubMed PMID: 24055410. PubMed PMCID: PMC4241465.
31. Zhu XH, Chen W. Observed BOLD effects on cerebral metabolite resonances in human visual cortex during visual stimulation: a functional (1)H MRS study at 4 T. *Magn Reson Med.* 2001;**46**(5):841-7. doi: 10.1002/mrm.1267. PubMed PMID: 11675633.
32. Chang WS, Liang WK, Li DH, Muggleton NG, Balachandran P, Huang NE, Juan CH. The association between working memory precision and the nonlinear dynamics of frontal and parieto-occipital EEG activity. *Sci Rep.* 2023;**13**(1):14252. doi: 10.1038/s41598-023-41358-0. PubMed PMID: 37653059. PubMed PMCID: PMC10471634.
33. Dimitriadis SI, Sun Y, Thakor NV, Bezerianos A. Causal Interactions between Frontal(θ) - Parieto-Occipital(α2) Predict Performance on a Mental Arithmetic Task. *Front Hum Neurosci.* 2016;**10**:454. doi: 10.3389/fnhum.2016.00454. PubMed PMID: 27683547. PubMed PMCID: PMC5022172.
34. Smucny J, Dienel SJ, Lewis DA, Carter CS. Mechanisms underlying dorsolateral prefrontal cortex contributions to cognitive dysfunction in schizophrenia. *Neuropsychopharmacology.* 2022;**47**(1):292-308. doi: 10.1038/s41386-021-01089-0. PubMed PMID: 34285373. PubMed PMCID: PMC8617156.
35. Tan PK, Tang C, Herikstad R, Pillay A, Libedinsky C. Distinct Lateral Prefrontal Regions Are Organized in an Anterior-Posterior Functional Gradient. *J Neurosci.* 2023;**43**(38):6564-72. doi: 10.1523/JNEUROSCI.0007-23.2023. PubMed PMID: 37607819. PubMed PMCID: PMC10513068.
36. Gratton C, Sun H, Petersen SE. Control networks and hubs. *Psychophysiology.* 2018;**55**(3):e13032. doi: 10.1111/psyp.13032. PubMed PMID: 29193146. PubMed PMCID: PMC5811327.
37. Wang M, Yang P, Wan C, Jin Z, Zhang J, Li L. Evaluating the Role of the Dorsolateral Prefrontal Cortex and Posterior Parietal Cortex in Memory-Guided Attention With Repetitive Transcranial Magnetic Stimulation. *Front Hum Neurosci.* 2018;**12**:236. doi: 10.3389/fnhum.2018.00236. PubMed PMID: 29930501. PubMed PMCID: PMC5999747.
38. Verkhratsky A, Schousboe A, Parpura V. Glutamate and ATP: The Crossroads of Signaling and Metabolism in the Brain. *Adv Neurobiol.* 2014;**11**:1-12. doi: 10.1007/978-3-319-08894-5_1. PubMed PMID: 25236721.
39. Bliss TV, Collingridge GL. A synaptic model of memory: long-term potentiation in the hippocampus. *Nature*. 1993;**361**(6407):31-9. doi: 10.1038/361031a0. PubMed PMID: 8421494.
40. Hancu I. Optimized glutamate detection at 3T. *J Magn Reson Imaging*. 2009;**30**(5):1155-62. doi: 10.1002/jmri.21936. PubMed PMID: 19856449. PubMed PMCID: PMC2783923.
41. Hancu I, Port J. The case of the missing glutamine. *NMR Biomed*. 2011;**24**(5):529-35. doi: 10.1002/nbm.1620. PubMed PMID: 21264975.
42. Di Maio V. The glutamatergic synapse: a complex machinery for information processing. *Cogn Neurodyn*. 2021;**15**(5):757-81. doi: 10.1007/s11571-021-09679-w. PubMed PMID: 34603541. PubMed PMCID: PMC8448802.
43. Le Ray D, Cattaert D. Active motor neurons potentiate their own sensory inputs via glutamate-

induced long-term potentiation. *J Neurosci.* 1999;**19**(4):1473-83. doi: 10.1523/JNEUROSCI.19-04-01473.1999. PubMed PMID: 9952423. PubMed PMCID: PMC6786021.

44. Kodama T, Hikosaka K, Watanabe M. Differential changes in glutamate concentration in the primate prefrontal cortex during spatial delayed alternation and sensory-guided tasks. *Exp Brain Res.* 2002;**145**(2):133-41. doi: 10.1007/s00221-002-1084-y. PubMed PMID: 12110952.
45. Hu Y, Chen X, Gu H, Yang Y. Resting-state glutamate and GABA concentrations predict task-induced deactivation in the default mode network. *J Neurosci.* 2013;**33**(47):18566-73. doi: 10.1523/JNEUROSCI.1973-13.2013. PubMed PMID: 24259578. PubMed PMCID: PMC3834059.
46. Schüler A, Scheiter K, Van Genuchten E. The role of working memory in multimedia instruction: Is working memory working during learning from text and pictures? *Educational Psychology Review.* 2011;**23**:389-411. doi: 10.1007/s10648-011-9168-5.
47. Li Q, Gong D, Tang H, Tian J. The neural coding of tonal working memory load: An functional magnetic resonance imaging study. *Front Neurosci.* 2022;**16**:979787. doi: 10.3389/fnins.2022.979787. PubMed PMID: 36330345. PubMed PMCID: PMC9623178.
48. Squire LR. Memory and brain systems: 1969-2009. *J Neurosci.* 2009;**29**(41):12711-6. doi: 10.1523/JNEUROSCI.3575-09.2009. PubMed PMID: 19828780. PubMed PMCID: PMC2791502.
49. Yoon JH, Grandelis A, Maddock RJ. Dorsolateral Prefrontal Cortex GABA Concentration in Humans Predicts Working Memory Load Processing Capacity. *J Neurosci.* 2016;**36**(46):11788-94. doi: 10.1523/JNEUROSCI.1970-16.2016. PubMed PMID: 27852785. PubMed PMCID: PMC5125231.
50. Kreutzwiser D, Tawfic QA. Expanding Role of NMDA Receptor Antagonists in the Management of Pain. *CNS Drugs.* 2019;**33**(4):347-74. doi: 10.1007/s40263-019-00618-2. PubMed PMID: 30826987.
51. Mei YY, Wu DC, Zhou N. Astrocytic Regulation of Glutamate Transmission in Schizophrenia. *Front Psychiatry.* 2018;**9**:544. doi: 10.3389/fpsyt.2018.00544. PubMed PMID: 30459650. PubMed PMCID: PMC6232167.
52. Bear MF, Abraham WC. Long-term depression in hippocampus. *Annu Rev Neurosci.* 1996;**19**:437-62. doi: 10.1146/annurev.ne.19.030196.002253. PubMed PMID: 8833450.